

Analysis of the Dynamic Behavior of Actual and New Design Solutions for Motorcycles using the multibody codes of MSC.visualNastran

Paolo Lista

Lista Studio srl , via Costa, 36 – 36030 Fara Vicentino Vi (Italy)
tel. +39,0445,300391 fax +39,0445,874283 www.lista.it www.mscsoftware.it

Vittore Cossalter, Roberto Berritta, Francesco Biral, Stefano Garbin

Department of Mechanical Engineering
University of Padua (Italy)

Abstract

In the last few years the automotive and motorcycle industries, pressed by the need for better rider safety, have shown an increasing interest in the simulation of the dynamic behaviour of actual and innovative vehicles.

In this paper an evaluation method of motorcycle handling is presented using the multibody code visualNastran by MSC Working Knowledge. In addition, this paper focuses also on a new three-wheeled vehicle concept developed with this approach.

The mathematical tyre model that calculates contact forces and torques between road surface and tyres, allowing multibody analysis of motorcycle dynamics, is first presented. The rider code and look-ahead path follower that have been developed at Padua University to simulate real driving situation are then discussed. Data obtained simulating an Aprilia RSV 1000 motorcycle virtual model in different situations, such as constant radius turns, constant camber angle turns and slaloms at various speeds, are exposed and compared to the data recorded on the real vehicle driven in the same manoeuvres. Subsequently, data obtained from simulations are analysed to define relationships and transfer functions between dynamic and cinematic variables defining motorcycle behaviour. Movies of the same approach, applied also to Moto Guzzi and Harley Davidson motorcycles, will be shown during the paper presentation.

The second part of this paper deals with a three-wheeled vehicle, which is a fine synthesis between the manoeuvrability and compactness of a motorcycle and the stability and load-bearing capacity of a four-wheeled car.

The solution presented is characterised by the innovative patented system of linking the rear frame to the front frame so that the latter tilts like motorcycles do whereas the rear frame does not. The linking system is a four bar linkage whose geometry can be adjusted to set the position of the instant tilting axis of the front frame with respect to the rear one closer to or further from the road surface. Moreover, it is possible to vary the inclination of the tilting axis on the longitudinal plane. A model of this vehicle was developed using the visualNastran multibody software by MSC. Different analyses have been carried out varying the geometrical parameters of the linking system in order to find the best handling and safety behaviour. Finally, a real working prototype of the vehicle was built. As in the virtual model, the prototype can change the geometry of the linking system. Different test drivers have accomplished many manoeuvres with different geometrical configurations. These tests confirmed the predicted simulations results.

First part: evaluation method of motorcycle handling model

Among the various multibody codes available in the market, the choice of a model for the evaluation method of a motorcycle handling made for this work are the **MSC Working Model** and **visualNastran Motion**[®], chosen for their power and flexibility. (Fig. 9). The model is composed by several rigid bodies: front and rear wheel, rear fork, front unsprung components, front fork, frame and motor, driver.

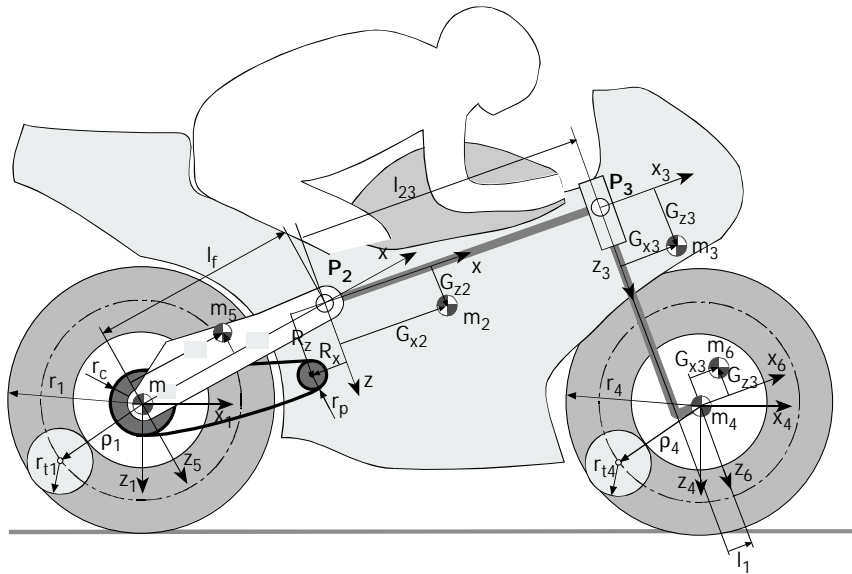


Fig. 1: components of the model

Mass, inertia properties and suspension characteristics are those declared by Aprilia; all of the unknown properties were measured at Padua University Laboratories.

“Easy Rider” code

The calculations of forces and torques acting between tyres and road surface, and the driving control, were implemented in a new software, called "Easy Rider" (Fig. 10). This software was written in **Visual Basic**[®] and linked to visualNastran Motion using OLE technology (Object Linking and Embedding).

Particularly at each integration step Easy Rider takes the position, orientation, linear and angular position of every wheel as inputs from visualNastran Motion, and gives forces and torques that are applied to the wheel hub as output.

Tyre’s mathematical model

This is the first fundamental part of the Visual Basic code implemented.

At every integration step visualNastran Motion passes to Easy Rider the positions and the linear and angular velocities of the wheels. By means of some coordinate changes, Easy Rider calculates the contact point between road surface and tyres, its absolute velocity (VP) and the same velocity without the rotational term (VT) (Fig. 2)

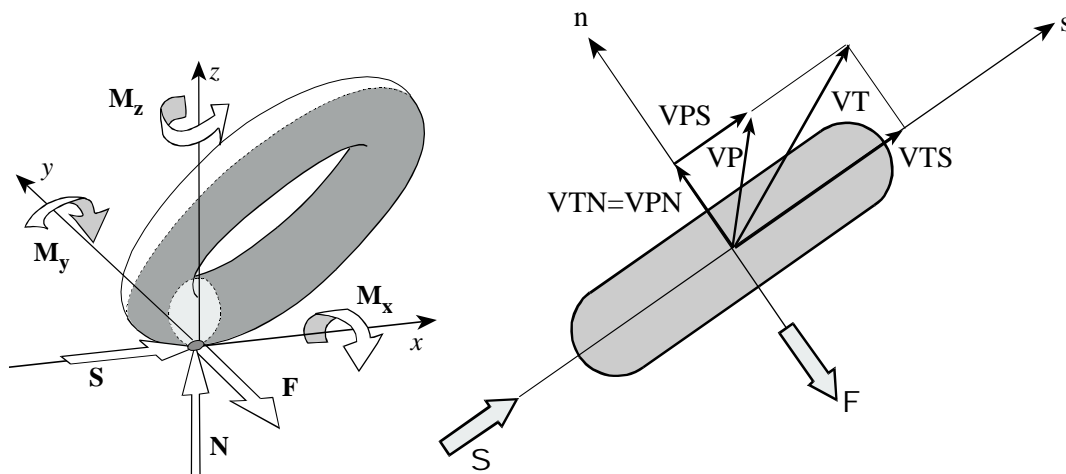


Fig. 2: tyre model

Longitudinal slip and sideslip angle are:

$$s = -\frac{VPS}{VTS} \quad \lambda = \arctan\left(\frac{VTN}{VTS}\right)$$

The knowledge of these parameters is necessary to calculate, by means of Pacejka's "magic formula", longitudinal and lateral forces. These forces are influenced by each other, and also by roll angle:

$$\sigma_x = \frac{s}{1+s} \quad \sigma_y = \frac{\lambda}{1+s} \cdot \frac{k_\phi}{k_\lambda} \cdot \phi \quad \sigma_{eq} = \sqrt{\sigma_x^2 + \sigma_y^2}$$

Vertical force depends on the compenetration (z) between tyre and road surface by means of tyre's stiffness (k_p) and damping (c_p).

$$N = k_p \cdot z + c_p \cdot \dot{z}$$

The coefficients B, C, D, E are strictly related to tyre's performance and are used to calculate longitudinal (S) and lateral (F) forces.

$$S = \frac{\sigma_x}{\sigma_{eq}} \cdot N \cdot D_{\ln g} \cdot \sin\left\{C_{\ln g} \cdot \arctan\left[B_{\ln g} \cdot \sigma_{eq} - E_{\ln g} \cdot \left(B_{\ln g} \cdot \sigma_{eq} - \arctan\left(B_{\ln g} \cdot \sigma_{eq}\right)\right)\right]\right\}$$

$$F = \frac{\sigma_y}{\sigma_{eq}} \cdot N \cdot D_{\ln t} \cdot \sin\left\{C_{\ln t} \cdot \arctan\left[B_{\ln t} \cdot \sigma_{eq} - E_{\ln t} \cdot \left(B_{\ln t} \cdot \sigma_{eq} - \arctan\left(B_{\ln t} \cdot \sigma_{eq}\right)\right)\right]\right\}$$

The lateral force reaches its maximum (F_0) value after laterally slipping of a certain length, which is called *relaxation length* (L_r). This equation shows that at higher speed lateral force reaches its maximum in a shorter time.

$$\frac{L_r}{V} \cdot \frac{d(F)}{dt} + F = F_0$$

Self-aligning torque depends on tyre's trail (t_0), sideslip angle and lateral force.

$$t = t_0 \cdot \left(1 - \left|\frac{\lambda}{\lambda_{\max}}\right|\right)$$

$$Mtz_{\text{trail}} = \begin{cases} t \cdot F_{\text{lat}} & t \geq 0 \\ 0 & t < 0 \end{cases}$$

Overturning torque depends on roll angle and vertical force.

$$Mtz_{\text{camber}} = mr \cdot \phi \cdot N$$

The total torque on Z vertical axis (perpendicular to road surface) is:

$$Mtz = Mtz_{\text{camber}} + Mtz_{\text{trail}}$$

The path control

The second fundamental part of Easy Rider is the control applied to the steer, which has to keep the balance of the motorbike-rider system and drive it along a particular path.

This kind of control is based on the "look ahead" technique.

What does it mean driving a vehicle? Looking ahead and trying to guess in which position the bike could be with respect to the path to be followed, and then applying a torque to the steer to reduce the previewed error.

The "look ahead" control behaves exactly in the same manner (Fig. 3): starting from motorbike's actual configuration (position and velocities of the centre of mass), it calculates in which position with respect to the trajectory the bike should be after a certain time "t". Using this distance "d", its derivative, roll angle and roll speed it calculates steering torque:

$$\tau = K_1 \cdot \varphi + C_1 \cdot \frac{d(\varphi)}{dt} + K_2 \cdot d + C_2 \cdot \frac{d(d)}{dt}$$

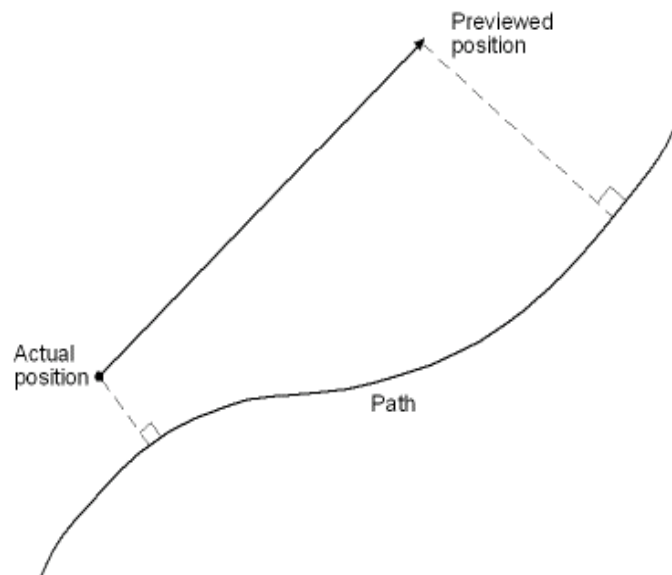


Fig. 3: the "look ahead" control

The path to be followed is defined by a parametric function $X = X(L)$, $Y = Y(L)$, where X and Y are the coordinates on the ground plane, L is the distance covered by the bike. To easily draw generic trajectories, a graphical tool called "track generator" has been developed: the path is composed by straight lines and arcs automatically joined to preserve the continuity of the first derivative (no singular points).

Comparisons between simulations and reality

The virtual prototype was involved in several standard manoeuvres, such as constant radius curves and slaloms at various speeds; the same thing was done with the real motorcycle, carrying a telemetry system.

Kinematical and dynamical data were measured and recorded; in the following graphs (Fig. 4) some of them are shown in the case of a constant radius of 7 m turn, at low speed (about 6.5 m/s).

In order, these graphs represent: steering angle, steering torque, yaw rate and roll angle; the correspondence between telemetry and simulations is very good: this indicates the accuracy of the model.

The thin dashed lines represent true telemetry values: road irregularities affect them strongly, so were also drawn thin continuous lines which represent smoother values.

For example, if steering torque has a negative value when the bike is turning right, a left torque to keep the balance is applied. Roll angle is positive when the motorbike leans right.

The next graphs (Fig. 5) show a slalom manoeuvre (pitch = 21 m, speed = 15 m/s): the quantities analysed are, in order: roll angle, roll speed, steering torque and yaw rate and versus time.

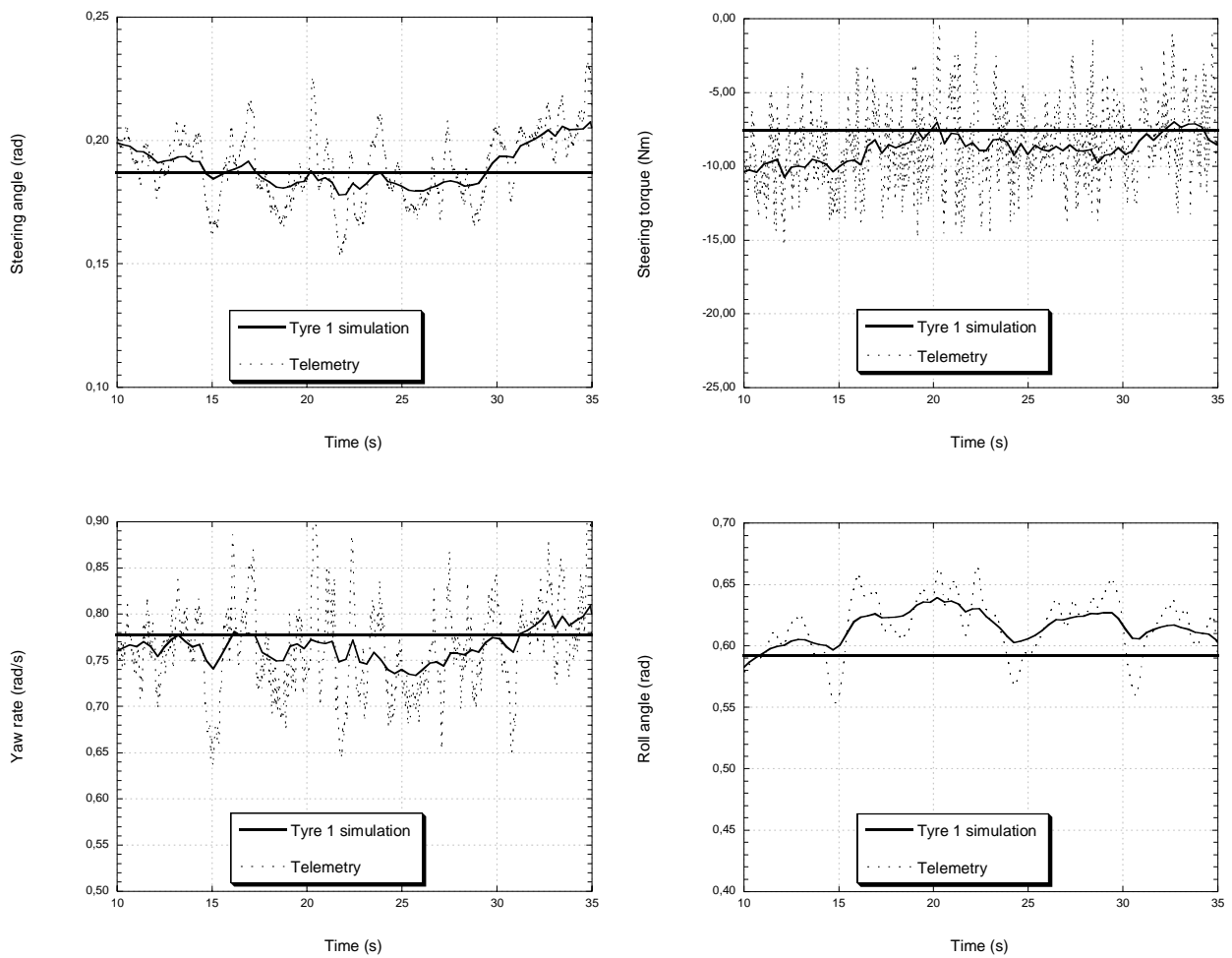


Fig. 4: simulation of a constant radius turn

The simulations were carried out using two different sets of data, one of them representing a racing tyre (tyre 1), the other a normal tyre (tyre 2). However, the difference between the two is very slight, because the manoeuvre is at low speed, not at the limit.

Also in this case the correspondence between simulations and telemetry is good.

The phase between steering torque (which can be considered the input quantity) and roll angle (output) has a negative value of about 90 degrees; roll angle and yaw rate are in phase; steering torque and roll speed have 180 degrees phase.

Considerations on handling properties

The virtual model was involved in a set of standard manoeuvres with both constant radius turn or constant roll angle, slowly increasing speed from 5 m/s up to the adherence limit. The aim of this choice was to keep the model almost in steady state, trying to find out some relationships between measured quantities and handling properties of the motorcycle.

In Fig. 6 steering torque is plotted versus speed, for different values of roll angle.

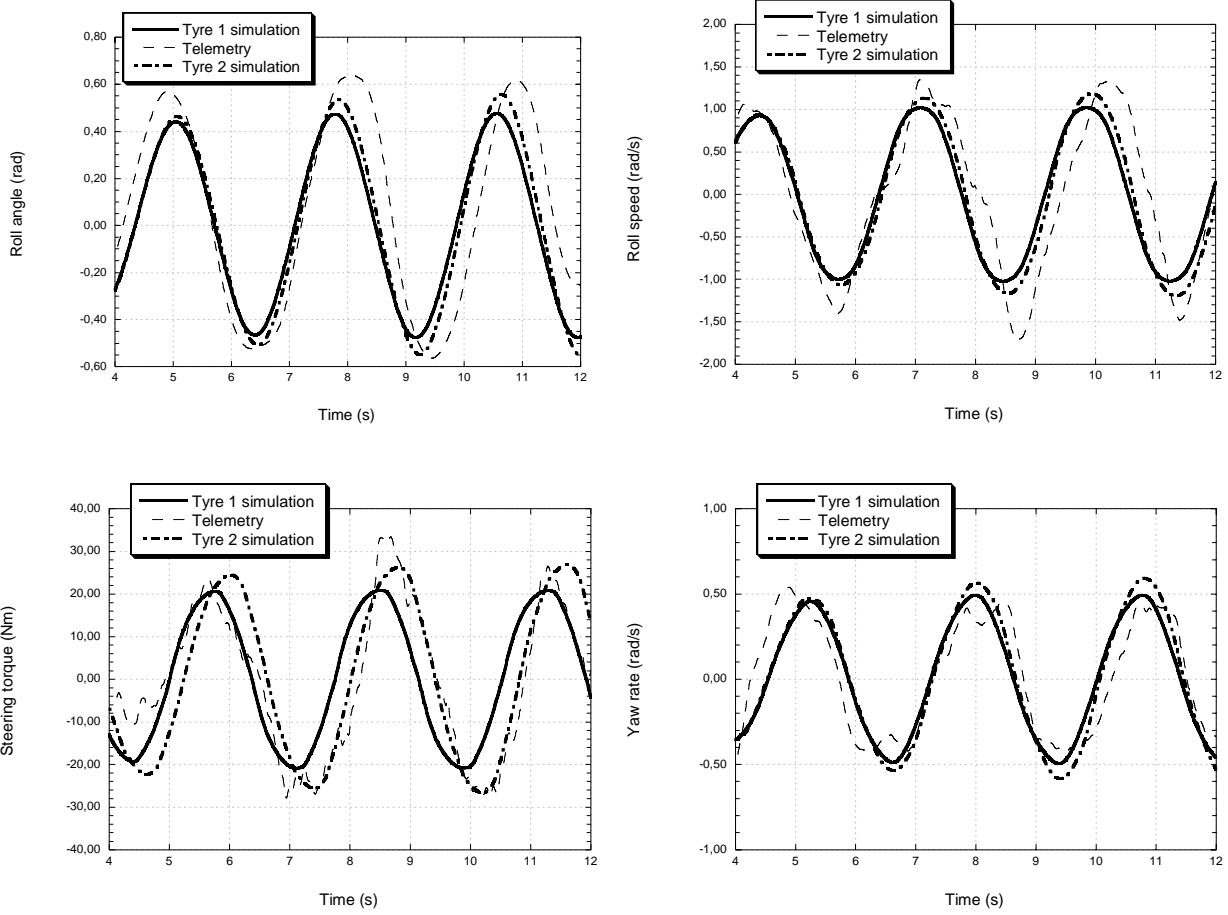


Fig. 5: simulation of a slalom

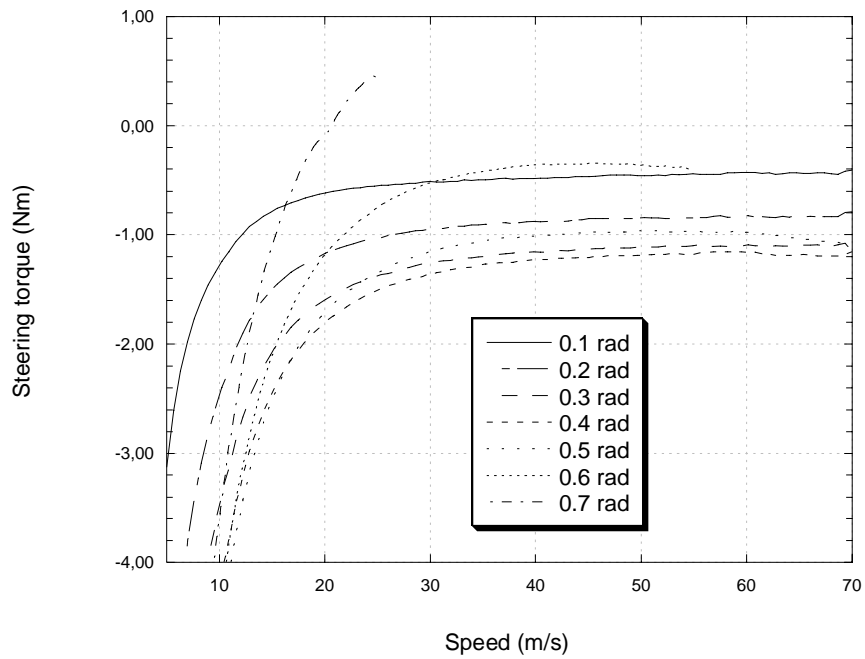


Fig. 6: steering torque vs. speed changing roll angle

The increasing of speed rapidly leads to less negative values: the lines referring to 0.6 rad and 0.7 rad suddenly stop, this means that the bike reaches its limit of adherence and falls. Steering torque values lay near zero when speed is greater than 15 m/s: keeping the balance requires very little effort.

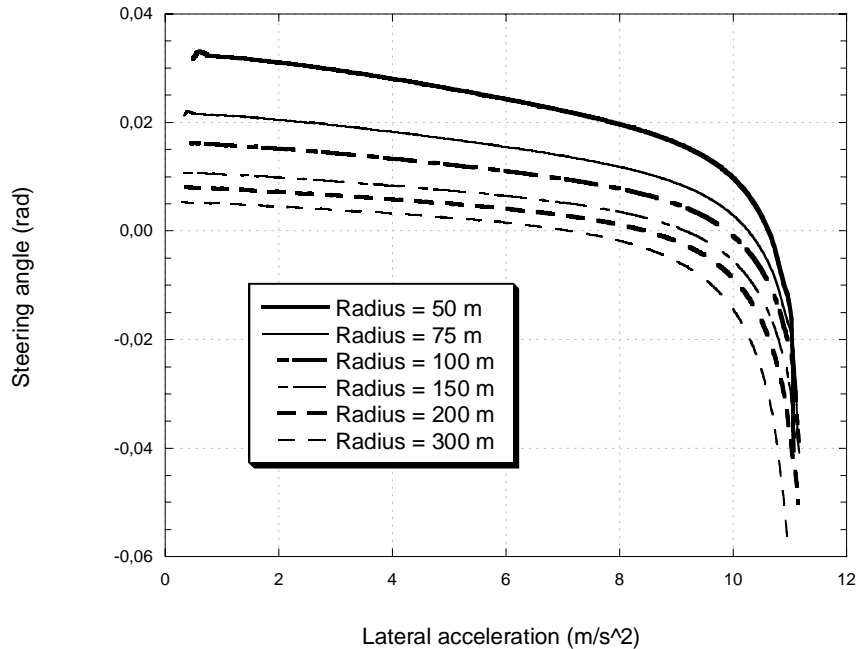


Fig. 7: steering angle vs. lateral acceleration changing path’s radius

The graph shown in Fig. 7 represents the variation of steering angle versus lateral acceleration (V^2/R) for different values of turning radius. The steering angle always decreases as speed increases; when its values are less than zero it means that the bike is driven in countersteering.

The maximum value for lateral acceleration is 11 m/s^2 in all cases: this is the limit for tyre’s adherence.

A very interesting parameter to understand motorbike's handling characteristics is the ratio between steering torque and lateral acceleration versus forward speed. As shown in Fig. 8, a particular family of curves (the dashed ones) which characterizes motorbike's geometric and inertial configuration is obtained. Diminishing caster angle (inclination of steering axis) by 5° causes a new line family to appear (the continuous ones). These lines are shorter than the old ones: this means that the modification has lead to a worst performance (the bike falls at lower speed). Moreover new lines are lower, and this fact indicates a loss of manoeuvrability.

Conclusions of the handling model

The virtual prototype presented in this paper shows that there is a good correspondence between simulations and reality, which was tested in several typical manoeuvres, such as constant radius turns and slaloms. It was also developed a new control, based on “look ahead” technique, to simulate running on real portions of road, obtaining interesting results concerning motorcycle's handling characteristics. All this was done by implementing a new software, Easy Rider, which is powerful and user-friendly, together with visualNastran Motion.

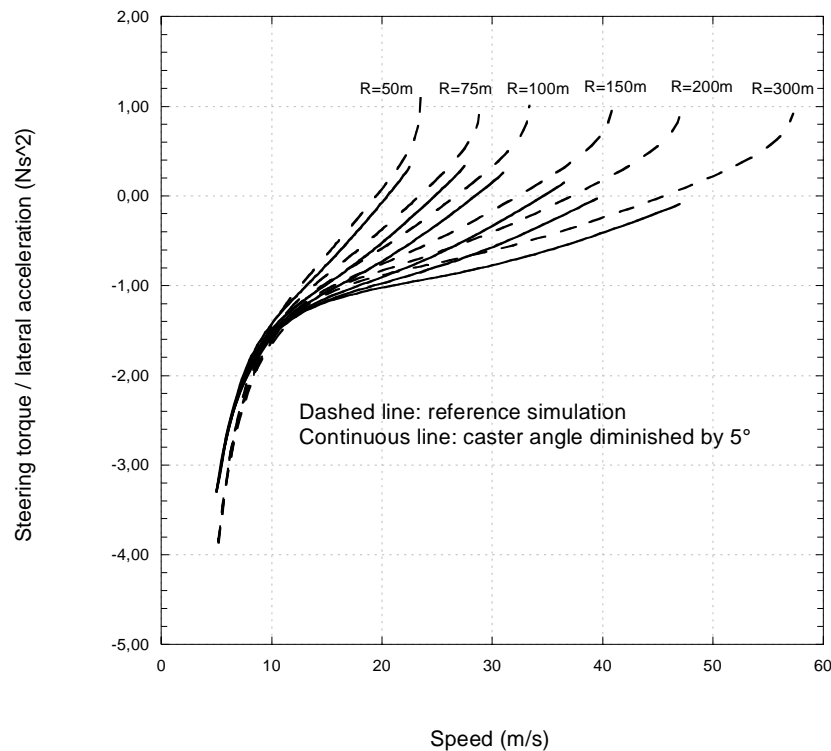


Fig. 8: ratio between steering torque and lateral acceleration vs speed

Second part: an innovative rolling vehicle

The handling model developed in the first part of this presentation turns to be extremely useful when applied to the design of a new vehicle.

A new solution of a motorcycle derived vehicle, where the driver controls the roll motion of the vehicle without the aid of any system, is here presented. The innovative feature of this vehicle is the system linking the front frame to the rear frame [21].

The aim of this work is to examine the dynamic behavior of the proposed vehicle and, in particular, the effects of the linking system. The influence of the four-bar geometry on the kinematic and dynamic behavior is investigated and some results are discussed.

Finally a comparison between the numerical results and the judgments of the test drivers about the prototype is proposed.

Vehicle description

This vehicle was first conceived, designed and simulated using virtual prototyping and then a prototype was built. First, the kinematic behaviour of the vehicle is presented and discussed, because it has a large influence on the vehicle's dynamic performance. Then the dynamic simulation results are shown and compared to the experimental results obtained from the driving tests using the prototype.

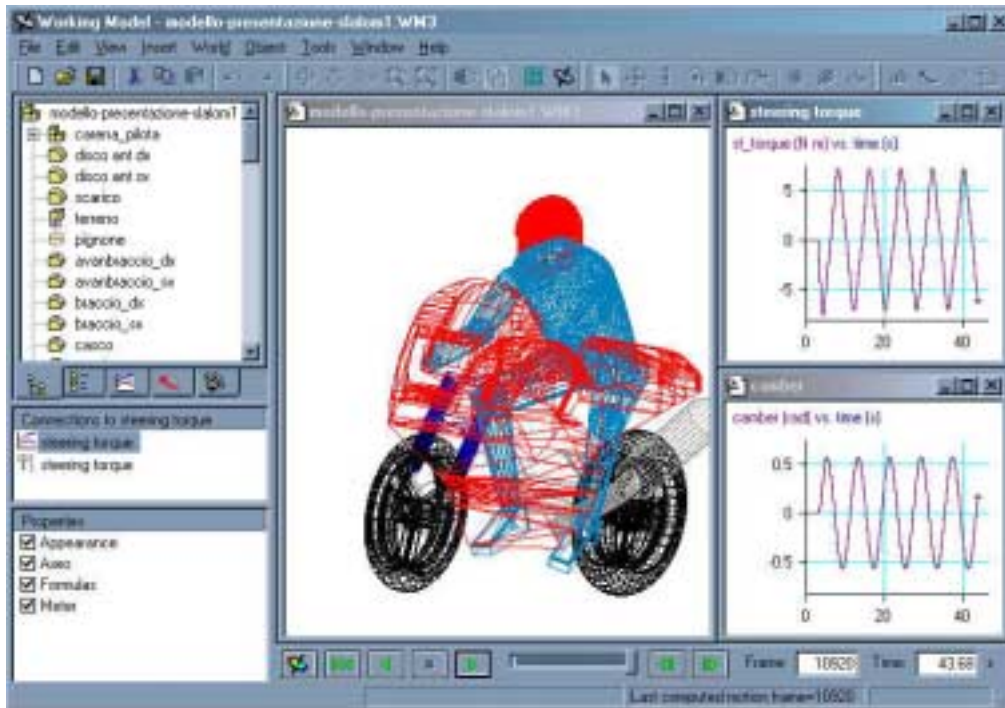


Fig. 9: MSC visualNastran Motion

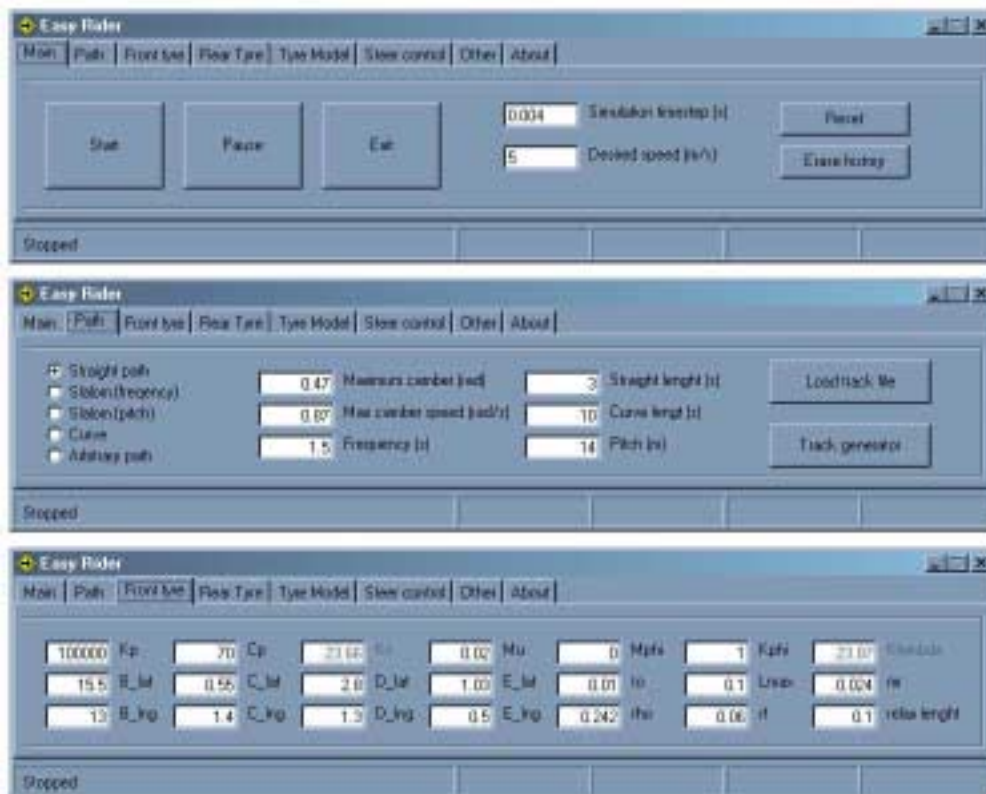


Fig. 10: Easy Rider software interface

This vehicle is characterized by three main assemblies. The first one is the rear assembly, which consists of the rear frame, two wheels, the engine and the rear suspension. The second assembly is the tilting front frame, which consists of the front wheel, the front fork and the suspension. The rear frame and the front frame are connected with a four bar linkage. This linkage is the innovative aspect of this vehicle and it is significantly responsible for the vehicle's dynamic behaviour.

The four-bar linkage is made up of the rear frame which do not tilt, the tilting front frame and two connecting bars that link the front and rear frame by means of four revolute-joints, which have the same axis orientation (Fig. 11).

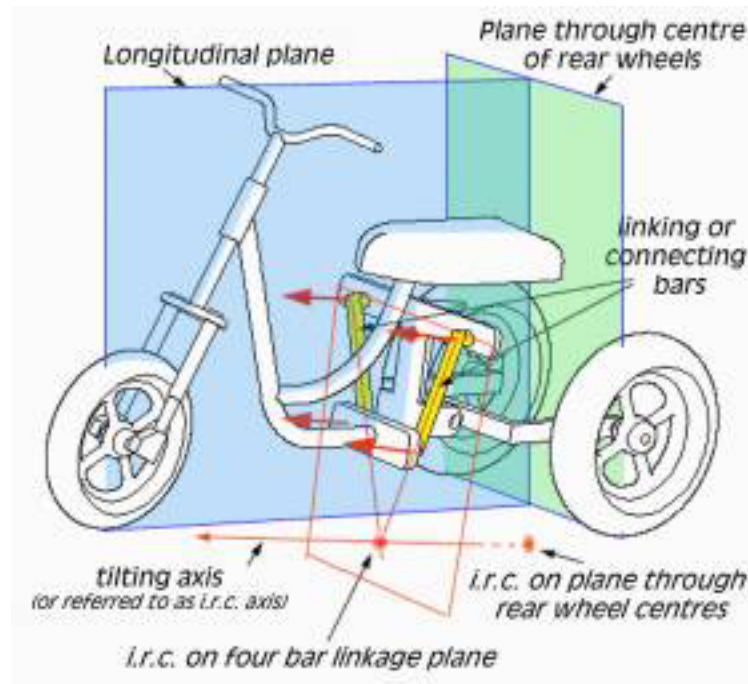


Figure 11: i.r.c. and rolling axis definitions

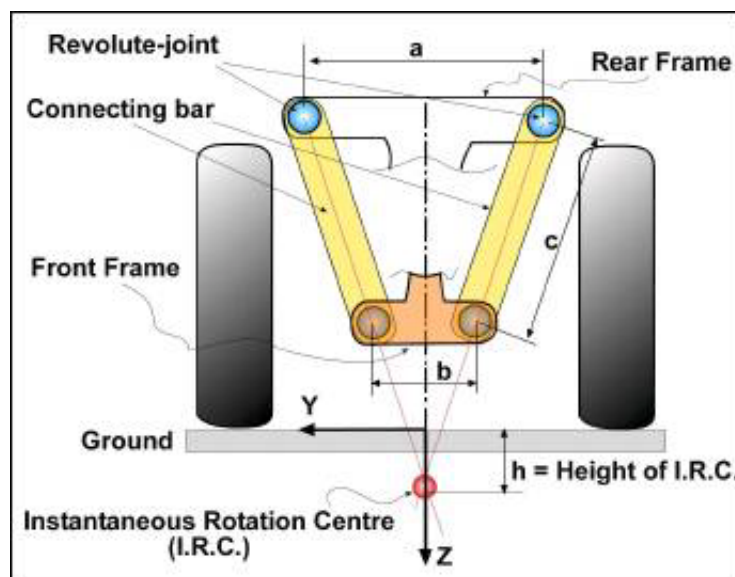


Figure 12: Four bar linkage elements

With this configuration the front frame rotates around an instantaneous tilting axis.

The intersection of the tilting axis with the four bar linkage plane defines the instantaneous rotation centre (referred to as *i.r.c.*). The *i.r.c.* position in the linkage plane is defined by the intersection of the two axes of the connecting rod, as shown in Fig. 12.

Hence, the distance a between the two superior revolute-joints, the length c of the connecting bars and the distance b between the two inferior revolute-joints (Fig. 12), define the instantaneous rotation centre position. Height h is defined as the vertical distance between road plane and *i.r.c.*; its value is positive when the *i.r.c.* is above the road plane, negative if the *i.r.c.* is below the road plane.

The instantaneous tilting axis can be moved up and down with respect to the road surface by decreasing or increasing the distance between the revolute-joints (parameters a and b) as shown in Fig. 13. As in general, the instantaneous tilting axis is not parallel to the road plane, when it moves up and down, and its intersection with the road plane moves back and forth.

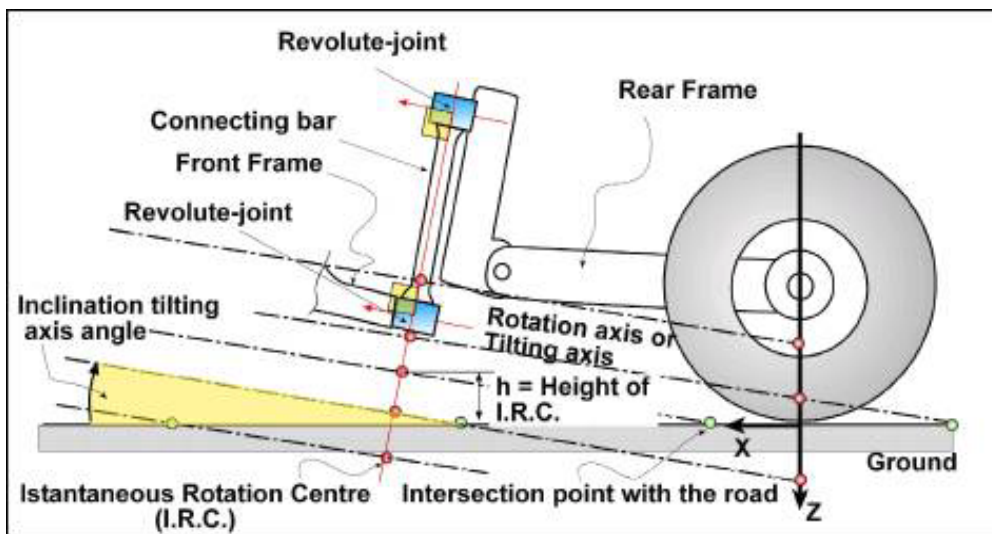


Figure 13 – Tilting axis vertical translation

It is also possible to fix the position of the *i.r.c.* (its height from the ground, parameter h) and rotate the tilting axis around this point changing the orientation of all the revolute-joint axes (see Fig. 14). Again, the intersection with road plane moves back and forth, except the case with the axis parallel to the ground. In this case there is no intersection at all.

All these possible configurations can be gathered into three main groups: the *i.r.c.* positioned over the ground (parameter h positive), on the ground (parameter h equal to zero), or under the ground (parameter h negative). These three different configurations influence significantly the dynamic behaviour of the vehicle.

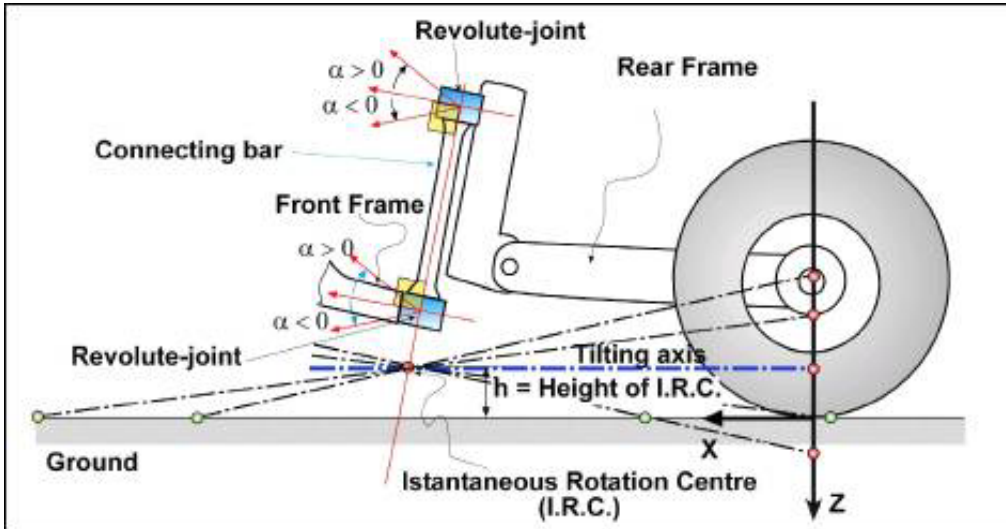


Figure 14 – Tilting axis rotation about i.r.c. on four bar linkage plane

The above mentioned kinematic considerations are based on the hypothesis that the vehicle is in its vertical position. When the front frame tilts towards one side, the *i.r.c.* moves towards the same side and height h from the road plane changes. If the *i.r.c.* is above the road, its distance from the road surface increases when the vehicle tilts. On the contrary, if the *i.r.c.* is under the ground its distance from the road surface decreases; in some cases the *i.r.c.* can even shift over the ground (Fig. 15).

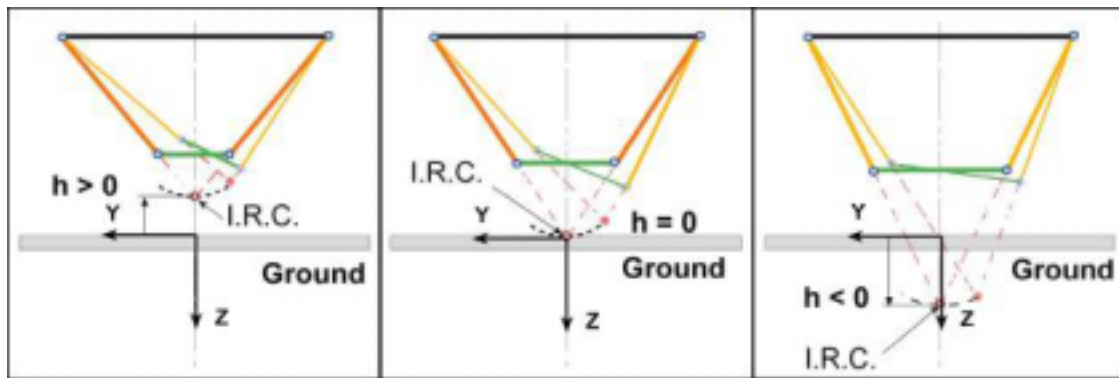


Figure 15 – Main four bar linkage possible configurations

The vertical and lateral position of the *i.r.c.* and the tilting axis inclination affect the load transfer from the inner rear wheel to the external rear one during a curve.

The equilibrium of the torques of the forces acting on the rear frame, with respect to the *i.r.c.* point, gives the load transfer ΔN , between the rear wheels, as a function of the position of the *i.r.c.* and of the centre of mass of the rear frame.

$$\Delta N = \frac{(g \cdot m - 2N) \cdot y_{i.r.c.} + m \frac{V^2}{R} (z_{cm} - h) + (F_l + F_r) \cdot h}{L}$$

where $y_{i.r.c.}$ is the lateral displacement of the *i.r.c.*, z_{cm} is the vertical position of the rear mass centre, F_l and F_r are the lateral forces on the rear wheels and $2N$ is the total vertical load on the rear wheels in static condition.

The forces transmitted by the connecting bars from the front frame to the rear frame do not give any contribution to the momentum because they pass through the *i.r.c.*

It is possible to observe that the load transfer depends both on mass forces (centrifugal and gravity) and on tyre lateral forces.

The more the *i.r.c.* is closer to the centre of mass the more the contribution of the centrifugal forces diminishes, but on the other hand the influence of the tyre lateral force increases its importance. The contrary happens if the *i.r.c.* is under the road surface because the momentum of the lateral forces changes sign.

Summarising, three relevant cases have to be investigated: the *i.r.c.* over the ground, on the ground and under the ground. Of course the effect of the inclination of the tilting axis has its own importance in all the three cases.

The Virtual Model

The components of the virtual vehicle were modelled and assembled using a standard CAD, which can be integrated in the multibody program visualNastran Motion.



Figure 16 – Tricycle virtual model screenshot made with visualNastran Motion

Exploiting the CAD associativity, it was possible to change the design parameters of the vehicle in the drawing environment and get the model updated automatically in the multibody software.

VisualNastran Motion lacks of a tyre model, thus it was necessary to use the motorcycle tyre model described in the first part of this paper. This tyre model represents the reactions of the road surface on the tyre by means of three torques (overturning, rolling resistance and yaw torques) and three forces acting on the geometric contact point.

It was also necessary to add the driver model capable to follow a given path, a simplified version of the “Easy Rider” described before. This was accomplished with a proportional derivative and integrative control. The tyre and driver model codes were written in Visual Basic and used the OLE technology (Object Linking Embedding) to send inputs (such as tyre forces, engine, brake and steering torques) and retrieve the vehicle motion state from visualNastran Motion.

Different kind of manoeuvres typically used for handling tests can be selected like U turn, steady state turn, lane change and slalom test.

Simulation results

The simulations were carried out considering principally U turns because these manoeuvres highlight the effect of the load transfer between the two rear wheels. The load transfer is important because it influences the total lateral adherence of the vehicle. In particular during a curve at very high speed or during obstacle avoiding manoeuvre, the load transfer may be so large that the internal wheel vertical load becomes equal to zero and the wheel rises from the road surface. This situation should be avoided to prevent rear frame roll over.

In addition, the U turn manoeuvre is useful to analyse the behaviour of the vehicle on entry and exit a curve, and evaluate the general handling behaviour of the vehicle.

Simulations were grouped in three main configurations:

- *i.r.c.* over the ground
- *i.r.c.* on the ground
- *i.r.c.* under the ground

and for some cases the inclination α of the revolute joints of the four bar linkage (and consequently of the tilting axis) was changed from -5° to $+5^\circ$.

In the graph of Fig. 17 the vertical loads on the two rear wheels are shown for a vehicle having an horizontal tilting axis considering several values of height h (in the range $-0.15 \div 0.15$ m). It is possible to see that the vertical load on the internal wheel (internal with respect to the turning side) decreases less if height h decreases. When height $h = -0.150$ m the internal wheel is more loaded than the external one.

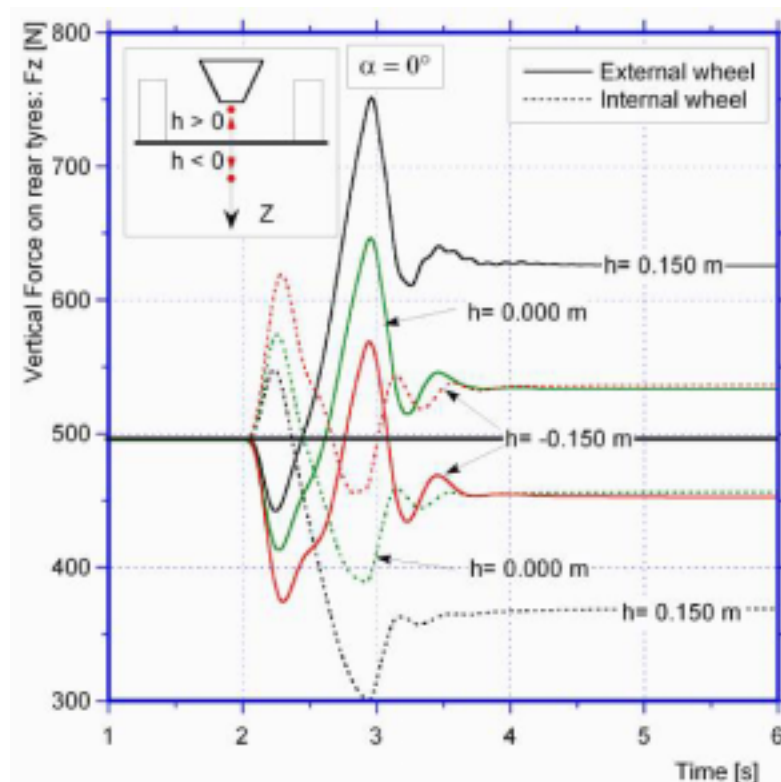


Figure 17 Load transfer between rear wheels varying h

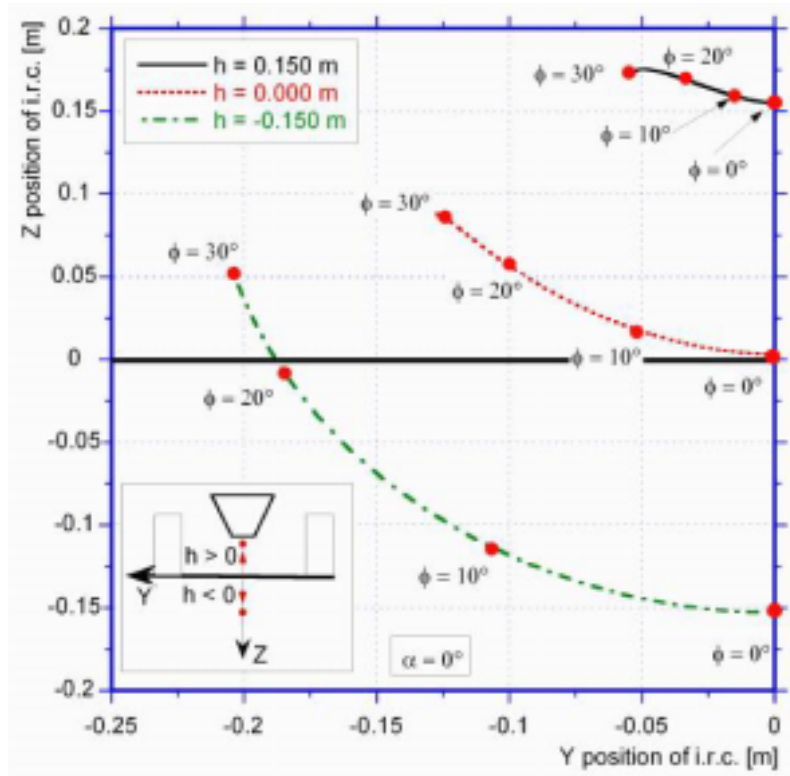


Figure 18– i.r.c. position varying h , for different roll angle values

In fact, as stated above, the load shift depends mainly on the position of the *i.r.c.* and on the position of the centre of mass of the rear frame. This phenomenon is better explained in Fig. 18, which depicts the trajectory of the *i.r.c.* on vertical plane y - z , as a function of the front frame roll angle ϕ . The more the *i.r.c.* is under the road plane the more the tilting axis shifts towards the internal wheel for a given roll angle. Moreover, for negative values of h , the *i.r.c.* moves vertically much more than for positive values of h .

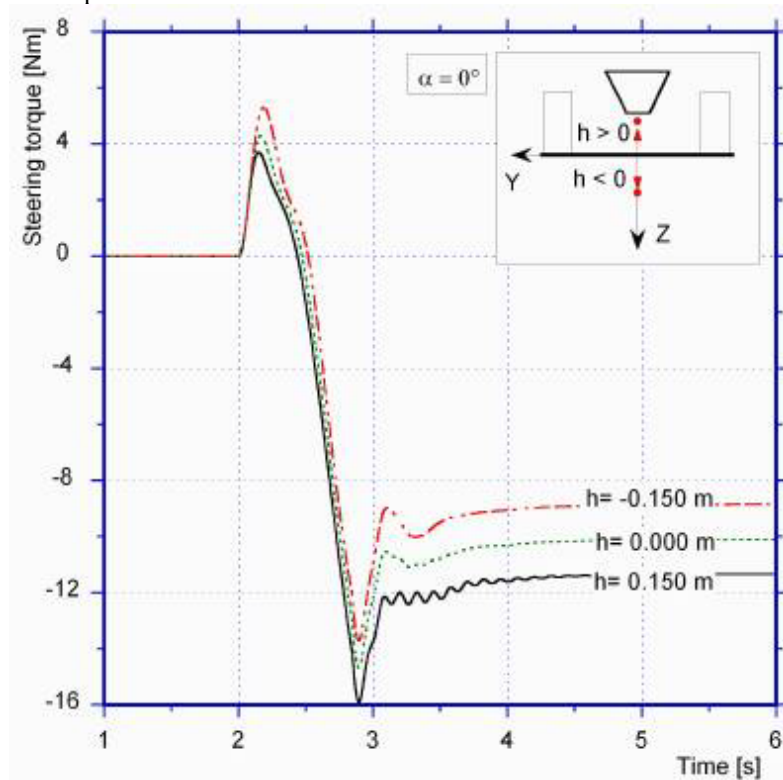


Figure 19 - Steering torque against time for different values of parameter h

In order to reduce the movements of the *i.r.c.* during tilting motion, it is necessary to shorten the connecting bar length c and to increase the length b . Then the effect of four bar linkage geometry on the steering torque is considered, because steering torque is closely related to vehicle handling.

The graph of Fig. 19 shows that when h decreases the absolute value of the steering torque in steady turning condition decreases, whereas the steering torque that the rider has to apply to begin the curve increases (e.g. the initial peak of the torque with h equals to -0.150 is greater than the peak of the torque with h equals to $+0.150$). This means that a configuration with the *i.r.c.* under the ground is more stable than the ones having the *i.r.c.* over the ground. Moreover, handling diminishes because a greater torque is required to tilt the front frame to perform a given manoeuvre.

The improvement of stability achieved with negative values of h is highlighted by the manoeuvre represented in Fig. 20 ($h = -0.30\text{m}$) in which the steering torque and the roll angle are plotted against time. The first part of the plot represents the entry in the curve followed by a steady turning condition. At time 4.5 s the rider suddenly stops exerting the steering torque and the vehicle returns to the vertical equilibrium configuration with small overshoots.

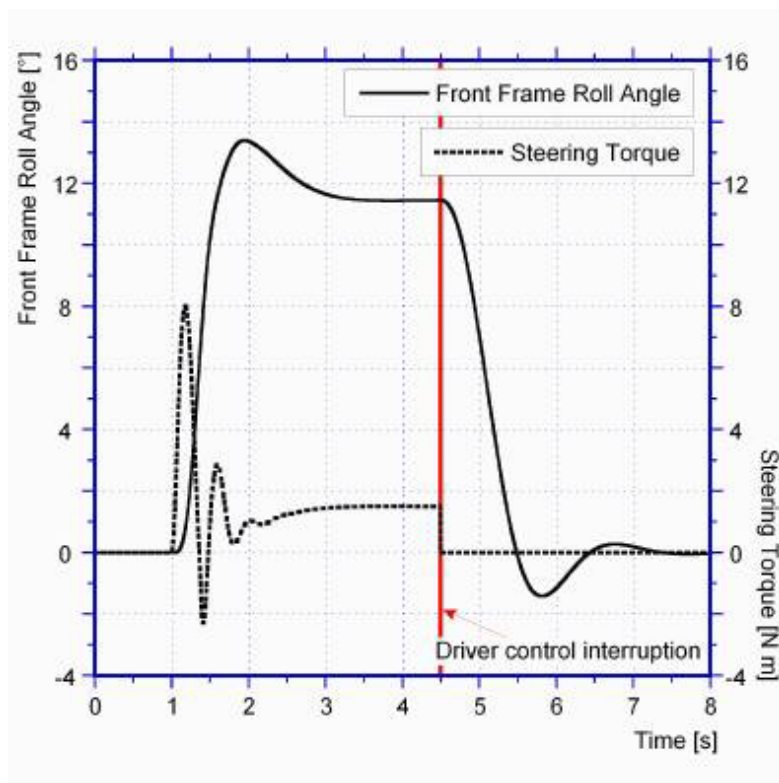


Figure 20 –Four bar linkage stable configuration

The angle of the axes of the revolute joints affects the orientation of the tilting axis and consequently the intersection of the tilting axis with the road plane. With positive angle α , the intersection with the road surface moves forwards and vice versa for negative values.

Figure 21 shows that the load transfer decreases when α increases.

The steering torque value is almost the same for different values of α , as it is shown in Fig. 22.

Other parameters that influence the steering torque and vehicle stability are tyre properties (and in particular the self-aligning torque and the twisting torque), castor angle and front fork offset which affect the vehicle trail [24], see Fig. 23.

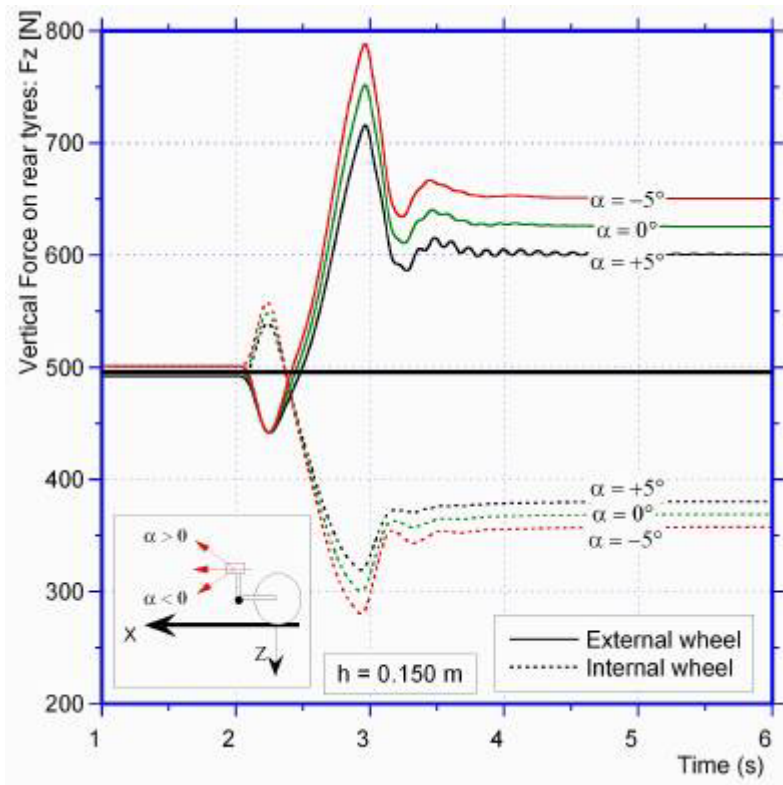


Figure 21 Load transfer between rear wheels varying α

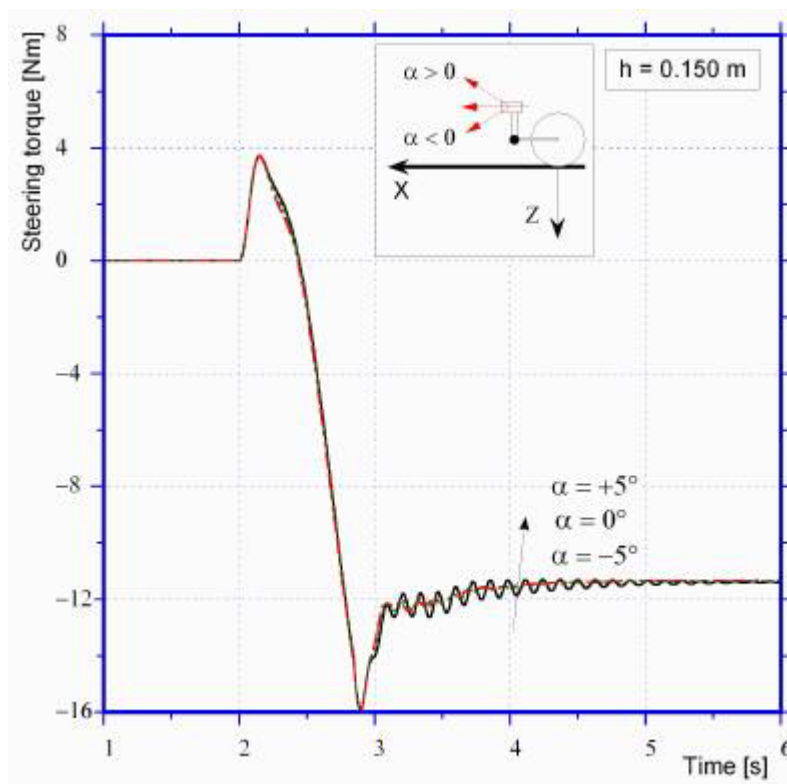


Figure 22 – Steering torque varying α

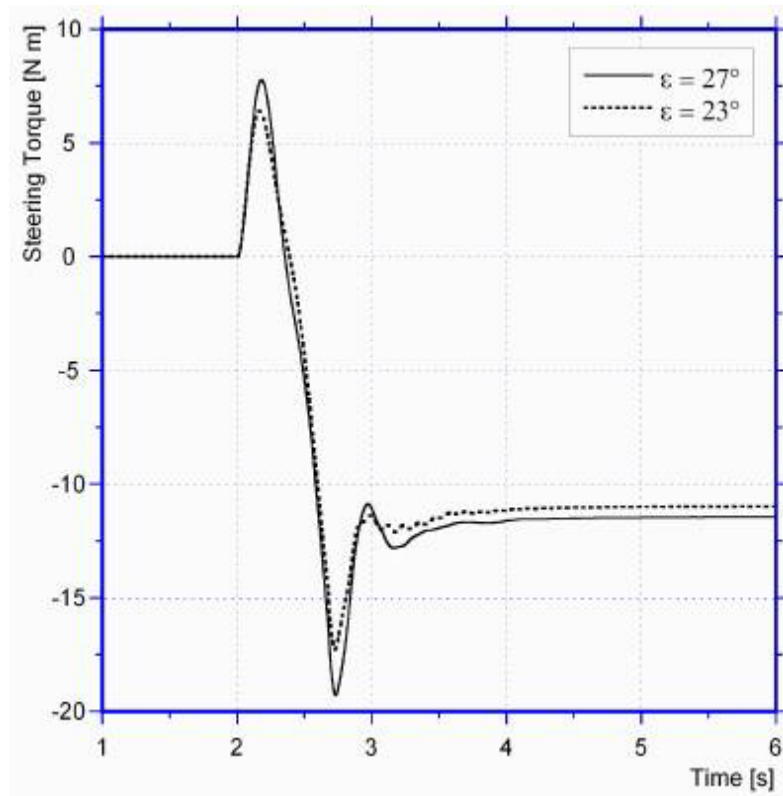


Figure 23 – Steering torque varying ϵ

The prototype

A working prototype based on the design parameters obtained from the simulation results was built (Fig. 24).



Figure 24 – Prototype during roll motion. Front and rear view.

As the virtual model the prototype four bar linkage geometry can be adjusted to achieve the desired set-up. This was accomplished creating a slot both in the rear and in the front frame in which the superior and inferior couple of revolute joints respectively can slide in order to obtain the assigned distance.

The length of the connecting bars can be varied screwing or unscrewing their ending part.

The inclination of the steering axis angle can be increased or decreased as well. Some test drivers carried out many tests with this prototype in different situations. Sometimes they tested limit manoeuvre in order to assess not only handling but also safety.



Figure 25 - Prototype built at the department. Revolute joints highlighted

Experimental results

The experimental tests yielded almost the same results that the simulations predicted.

The main handling and safety manoeuvres carried out were: obstacle avoidance, fast slalom, bump during turning manoeuvre and U turn manoeuvre, all these manoeuvres were performed with different four bar linkage configurations. The table 1 summarizes the results obtained, reporting the driver judgements.

A vehicle with a positive h parameter turned out to be faster during the obstacle-avoidance manoeuvre than the ones with negative h values. Moreover, it was necessary to apply a lower torque to tilt the front frame during transient period. On the other hand the three wheeled vehicle was more stable with the *i.r.c.* under the road surface, but the test driver found it more difficult to roll the front frame during curve entrance.

All these results agree with computer simulation.

	$h < 0,$ $\alpha = 0$	$h = 0,$ $\alpha = 0$	$h > 0,$ $\alpha = 0$	$h > 0,$ $\alpha > 0$
Steering torque effort	++	+	-	+
Handling	--	+	++	+++
Rear frame hopping effect	++	++	+	--
Rear and front frame coupling effect	--	--	--	++
Vertical Revolute joint effect	++	+	-	-

Table 1 – Test driver judgements for different four bar linkage configurations

The “*rear frame hopping effect*” phenomenon rises when the driver applies a particular high frequency sinusoidal steering angle in order to make the rear frame to hop. This effect disappears almost completely when the rolling axis is inclined.

The test driver felt what we called “*vertical revolute joint effect*” as a negative effect. This happens when the rear frame and front frame seems to be linked by a vertical revolute joint during the turning manoeuvre. This behaviour disappears almost completely when the angle of the tilting axis is positive.

But with a positive tilting axis angle another undesired phenomenon rises. This fact consists of a sort of coupling between rear and front frame. Any perturbation that occurs on the rear frame propagates to the front frame and the driver feels this phenomenon quite disturbing.

Conclusions on the innovative vehicle

A first series of studies were carried out on a three-wheeled vehicle having a tilting front frame. The vehicle was modelled by means of a 3D software and simulated with the aid of the multibody code visualNastran Motion. The influence of the four bar linkage, which connects the rear frame to the front frame, on the dynamic behaviour was deeply investigated.

The simulation results revealed the importance of the vertical position and inclination of the tilting axis on the load transfer between the rear wheels and on the steering torque that must be applied to do a curve.

The numerical results gave a contribution to the design and manufacturing of a working prototype that was tested in many different manoeuvres. A good agreement between simulation and experimental results was found.

The tests pointed out also some riding sensations that helped to understand the dynamic behaviour of this innovative vehicle.

Moreover, the prototype showed that it is possible to obtain substantial different vehicle performance simply varying the geometrical parameters of the four bar linkage, as predicted by the multibody model.

Aknowledgements

Special thanks to all the assistants and researchers at Department of Mechanics at Padua University, Italy, and especially to prof. Vittore Cossalter, enthusiast leader of all these efforts.

Appendix

In Fig. 26 the main vehicle dimensions used to carry out computer simulations are shown.

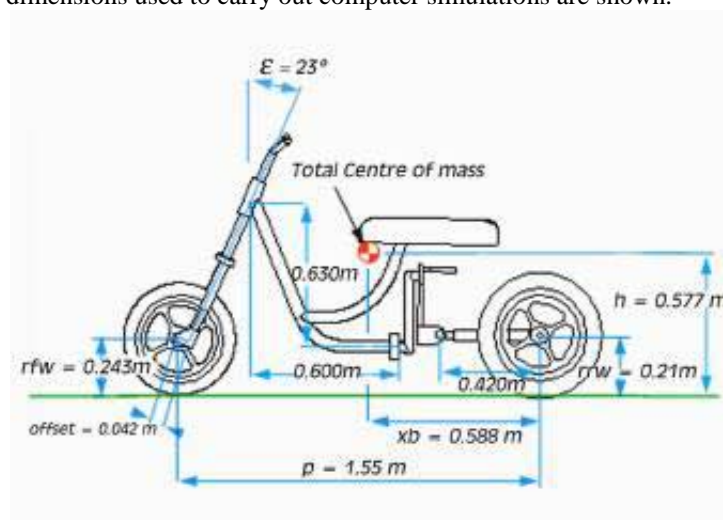


Figure 26- Tricycle main dimensions

Table 2 represents the mass properties of the main elements of the tricycle used during computer simulations.

	<i>Mass [kg]</i>
Connecting bar	3.5
Front fork	12
Front frame	12
Rear left wheel	2.8
Rear right wheel	2.8
Front wheel	3
Rear frame	45
Tank	6
Man	70

Table 2 – Masses of model elements

In Table 3 the four bar linkage different geometrical configuration used for the computer simulations are shown.

Configuration N°	Four bar linkage geometrical parameter				i.r.c. position
	<i>a</i> [m]	<i>b</i> [m]	<i>c</i> [m]	α [°]	<i>h</i> [m]
<i>Case 1</i>	0.500	0.090	0.320	0	0.155
<i>Case 2</i>	0.440	0.160	0.320	0	0.003
<i>Case 3</i>	0.400	0.200	0.320	0	-0.150
<i>Case 4</i>	0.500	0.090	0.320	+5	0.155
<i>Case 5</i>	0.500	0.090	0.320	-5	0.155
<i>Case 6</i>	0.380	0.240	0.320	0	-0.390

Table 3 – Four bar linkage geometrical configurations used for simulation

Case 1 to 5 have the geometrical dimensions shown in Fig. 26, while case 6 uses a different steering angle inclination ($\epsilon = 27^\circ$) and a different offset (0.025m instead of 0.042m).

References

- [1] V. Cossalter, Cinematica e dinamica della motocicletta, Edizioni Progetto, Padova, 1999
- [2] V. Cossalter, M. Da Lio, A. Doria, Meccanica applicata alle machine, Edizioni Progetto, Padova, 1995
- [3] AAVV, Motorcycle dynamics and rider control, SP-428 SAE, Warrendale, 1978
- [4] H. B. Pacejka, Tyre model for vehicle dynamics analysis, Swet & Zeitlenger, Amsterdam, 1991
- [5] D. H. Weir, J. W. Zellner, Development of handling test procedures for motorcycles, SAE 780313, 1978.
- [6] R. S. Sharp, Design for good motorcycle handling qualities, SAE paper n° 972124, 1997
- [7] T. Katayama, T. Nishimi, A simulation model for motorcycle riders's control behaviours, SAE 972126
- [8] H. Ishii, Y. Tezuka, Considerations of turning performance for motorcycles, SAE paper n° 972127, 1997
- [9] Y. H. Cho, J. Kim, An improved handling model of a driver/vehicle system..., ASME vol. n° 38, 1992
- [10] T F. Schweers, D. Remde, Objective Assessment of motorcycle maneuverability SAE n° 931551, 1993
- [11] La Brie E. G. - Patent No. US3561778: Three Wheeled Vehicle -1968

- [12] Patin P. - Patent No. US3781031: Three Wheeled Vehicles having Static and Dynamic Equilibrium - 1972
- [13] Hamamatsu JA. et al. - Patent No. US3995875: Tricycle - Suzuki Motor Company, Japan, 1974
- [14] Kensaku et al. - Patent No. US3938609: Tricycle - Daihatsu Motor Company Limited, Japan, 1975
- [15] Winchell F. J. / Orchard Lake - Patent No. US4065144: Cambering vehicle - GM Corp., Detroit, MI, 1975
- [16] Kanno et al. - Patent No. US4159752: Tricycle -Yamaha, Japan, 1977
- [17] Yamamoto et al. – Pat. US4316520: Unilateral rear-drive type of three-wheeled vehicle - Honda, Japan, 1980
- [18] Sato et al. - Patent No. US4360224: Tricycle with two fore wheels - Yamaha, Japan, 1980
- [19] Kawasaki et al. – Pat. US4421194: Tubing assembly in mutually movable portions.... – Honda - 1982
- [20] Irimajiri et al. - Patent No. US4703824 Three-wheeled vehicle -1984
- [21] Katsuyoshi Kawasaki - Patent No. 4,541,501 : Articulated Tricycle - 1985
- [22] Edmund F.N. Jephcott, - Patent No. 44,660,853: Vehicle Body Tilting Mechanism - 1987
- [23] Doman; Trevor D., - Patent No. USD0322049: Articulated three wheel vehicle -1988
- [24] King Klopfenstein, - Patent No. 4,903,857: Leaning Vehicle with Centrifugal Force Compensation - 1990
- [25] Richards – Pat. US5248011: Three wheeled vehicle having driven front wheels and steerable rear wheel - 1992
- [26] Peter Owsen, - Patent No. 5,240,267:Tricycle - 1993
- [27] Doveri M. - Patent No. EP626307A1: Laterally-leaning three wheeled vehicle - 1993
- [28] Vidal Carlos C. – Pat.US5611555: Articulated balancer with an oscillating axle and having ... - 1994
- [29] Van Den Brink, Kroonen – Pat. EP796193A1/B1: Self-stabilising, directionally controllable vehicle ... - 1995
- [30] Braun, Dieter - Patent No. WO9849023A1: Multi-track curve tilting vehicle , Daimler-Benz, 1998
- [31] Cossalter V. – Pat. 01300175, EP99114532.7: Meccanismo per la realizzazione di un veicolo ... – 1999
- [32] Cossalter,V. : Implementation of a motorcycle tire model in a multibody code - Tire Technology Int. - 1999
- [33] Koch, J./ Experimentelle und analytische Untersuchungen des Motorrad-Farher Systems, Berlin 1978